

Transition Metal Ions as Efficient Catalysts for Vilsmeier–Haack Formylation of Hydrocarbons with Reagents: Kinetics and Mechanism

K. C. Rajanna¹ · Aneesa Ferdose² · K. Rajendar Reddy¹ ·
M. Arifuddin³ · M. Moazzam Ali²

Received: 20 August 2015 / Accepted: 3 December 2015 / Published online: 17 February 2016
© Springer Science+Business Media New York 2016

Abstract The Vilsmeier–Haack formylation reactions with hydrocarbons are sluggish in acetonitrile medium. The VH reactions follows second-order kinetics and affords formyl derivatives under kinetic conditions that are also irrespective of the nature of the oxychloride (POCl_3 or SOCl_2) used for the preparation of VH reagent along with DMF. However, the reactions undergo significant rate accelerations in the presence of transition metal ions such as Cu(II), Ni(II), Co(II) and Cd(II). Transition metal ion catalyzed VH formylation is explained through the formation of a mixed ligand complex of the $[\text{M(II)S(VHR)}]$ type prior to the rate determining rearrangement step, before yielding formyl derivatives of hydrocarbons.

Keywords Vilsmeier–Haack formylation · Hydrocarbons · Transition metal ions · Catalysts · Kinetics · Mechanism

1 Introduction

The Vilsmeier–Haack reagent is a versatile reagent in organic synthesis [1–14]. Formylation of organic compounds is an important reaction in organic synthesis, which can be achieved more conveniently under Vilsmeier–Haack conditions than with other procedures [15–17] such as the Reimer–Tiemann [15], Gattermann–Koch [16], and Duff methods [17]. Earlier publications from our laboratory reported certain kinetic and mechanistic aspects of formylation, cyclization, acetylation and benzylation under VH conditions in various

✉ K. C. Rajanna
kcrajannaou@yahoo.com

¹ Department of Chemistry, Osmania University, Hyderabad 500007, India

² Department of Chemistry, M. J. C. E. T., Hyderabad 500034, India

³ National Institute of Pharmaceutical Education and Research (NIPER), Hyderabad 500037, India

solvent media [11–14]. Over the years, transition metal ions have received enormous attention by synthetic, inorganic and physical organic chemists all over the world because of their proven ability as efficient homogeneous catalysts in organic synthesis dealing with different redox [18–32], photochemical [29], and substitution reactions such as hydrogenation [30], nitration [31] and formylation reactions [32]. Even though many results have been published in the literature showing the catalytic effects of transition metal based species in a variety of chemical reactions, not much work has reported on transition metal ion catalyzed kinetic studies of VH reactions [29]. In continuation of our ongoing research on synthesis, kinetics and mechanism of VH reactions, the authors performed a detailed kinetic study of transition metal ion catalyzed Vilsmeier–Haack formylation of aromatic hydrocarbons.

2 Experimental Details

2.1 Materials

Solvents such as acetonitrile and dichloroethane were of highest purity HPLC grade. Deionized water was further purified over acid dichromate and alkaline permanganate solutions before use. All the other chemicals used in this study (organic substrates such as hydrocarbons, phenols, and their substituted compounds) were procured from Sigma Aldrich Chemicals (Hyderabad, India) with highest purity (99 %). A carbonate-free sodium hydroxide stock solution was prepared according to standard procedures and the concentration was systematically checked by titration against potassium hydrogen phthalate. All the metal nitrates used in the present work were of Analytical Reagent (AR) grade of 99 % purity (S.D. Fine Chemicals Ltd., India). Stock solutions of metal nitrates (Cu(II), Co(II), Ni(II) and Cd(II) nitrates) were prepared in acetonitrile solvent and standardized by EDTA titrations according to literature procedures [33].

2.2 VH Reagents

Flasks containing DMF dissolved in a suitable solvent {generally dichloroethane (DCE), or acetonitrile (ACN)}, along with SOCl_2 and POCl_3 , were cooled and thermally equilibrated for about 30 min at $-5\text{ }^\circ\text{C}$ by keeping them in a benzene trough chilled from outside with ice and NaCl. Requisite amounts of solvent and amide were transferred into a 100 mL flask and POCl_3 or SOCl_2 was added drop wise, at $-5\text{ }^\circ\text{C}$, with constant stirring. The resultant reagent mixture was kept aside for about an hour to ensure complete formation of the VH adduct. Its concentration was checked by acid–base titration to the bromocresol green end point according to literature reports [9–14].

2.3 Kinetic Method

Organic substrates such as hydrocarbons, phenols, and their substituted derivatives were used for kinetic studies of VH reactions in ACN and DCE. The thermostat (Toshniwal, India) was adjusted to the desired reaction temperature (with a precision of $\pm 0.1\text{ }^\circ\text{C}$). Two different flasks, one containing known amount of Vilsmeier–Haack reagent (DMF/SOCl_2 or DMF/POCl_3) in a suitable solvent, and the other with the substrate solution, were taken and clamped in the thermostatic bath for about 30 min. The reaction was initiated by

adding the requisite amount of substrate solution to the reaction vessel containing the other contents of the reaction mixture. The entire reaction mixture was stirred until the end of the reaction. A kinetic method was adopted to monitor progress of the VH reaction, which is similar to that reported in our earlier papers [11–14]. Aliquots of the reaction mixture were withdrawn into a conical flask, containing considerable (and known) amount of hot distilled water, at different time intervals. The unreacted VH adduct underwent hydrolysis and gave a mixture of acids (hydrochloric and sulfuric acids for DMF/SOCl₂ and hydrochloric and phosphoric acids for DMF/POCl₃). The acid content was estimated against standard NaOH solution to the bromocresol green end point. Reproducibility of the results was crosschecked by conducting kinetic runs three to four times. The results were reproducible within $\pm 3\%$ error.

2.4 Product Analysis Under Kinetic Conditions

After completing the kinetic study of the reaction, excess (remaining part of the reaction mixture) was refluxed further and left aside overnight. The solution was then poured into ice-cold water with vigorous stirring and kept aside for about 2 h. The resultant solution was neutralized with sodium hydrogen carbonate. The organic phase was extracted with DCE, dried over MgSO₄ and the solvent evaporated. Products of the reaction were isolated and found to be formyl derivatives of the substrates (Scheme 1) as characterized by ¹H-NMR and mass spectra with comparison to authentic samples and found to be satisfactory (Table 1).

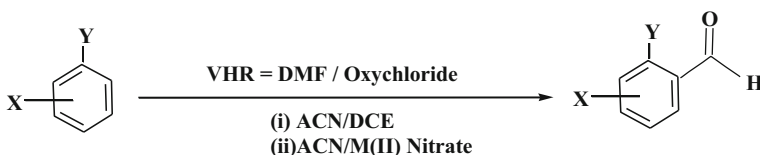
3 Results and Discussion

3.1 Order of the VH Reaction

Plots of $\ln V_t$ versus time were linear with negative slope and intercept as shown in Figs. 1 and 2, when $[\text{substrate}]_0 \gg [\text{VHR}]_0$ the reaction shows first-order kinetics in [substrate]. Representative data are presented in Table 2. However, under the condition $[\text{VHR}]_0 = [\text{substrate}]_0$, the plots of $[1/(a-x)]$ or $[1/V_t]$ versus time are linear with positive slope and intercept at the ordinate indicating that the VH reaction follows overall second-order kinetics (Figs. 3 and 4). From the slopes of these plots, second-order rate constant were evaluated.

3.1.1 Reactive Species of VH Adduct and Mechanism of Formylation Reactions Involving the DMF–Oxychloride [POCl₃ or SOCl₂] Adduct

In spite of different opinions prevailing on the formulae of the reactive VH adduct species, infrared spectroscopic studies of Arnold and Holy, electronic spectroscopic and ³¹P NMR spectroscopic study results of Marino, Martin and several others [3–10], together with the



Scheme 1 VHR = DMF + (SOCl₂ or POCl₃); Y = OH; X = ED or EWD groups

Table 1 Transition metal ion catalyzed VH (DMF/POCl₃) reactions with certain organic compounds

S. N	Substrate	Product	Conventional		Cu(II)		Ni(II)		Co(II)		Cd(II)	
			RT (h)	% Yield	RT (h)	% Yield	RT (h)	% Yield	RT (h)	% Yield	RT (h)	% Yield
1	Naphthalene	2-Naphthaldehyde	24	30	12	65	14	63	12	70	13	65
2	Phenol	2-Hydroxybenzaldehyde	24	30	10	80	10	82	10	85	10	78
3	4-Nitrophenol	5-Nitrosalicylaldehyde	24	18	16	65	18	60	16	60	16	60
4	2-Chlorophenol	3-Chlorosalicylaldehyde	24	20	18	70	16	55	15	62	18	60
5	<i>o</i> -Cresol	3-Methylsalicylaldehyde	24	35	10	72	12	70	10	70	12	75
6	<i>p</i> -Cresol	5-Methylsalicylaldehyde	24	32	10	74	12	75	12	75	12	78
7	Toluene	4-Methylbenzaldehyde	24	31	12	65	11	63	12	68	12	65
8	Anisole	4-Methoxybenzaldehyde	24	37	12	67	10	65	11	65	13	67
9	1-Naphthol	2-Formyl-1-naphthol	24	35	10	82	10	82	10	80	10	80
10	2-Naphthol	1-Formyl-2-naphthol	24	35	10	70	10	65	10	65	10	65

RT room temperature

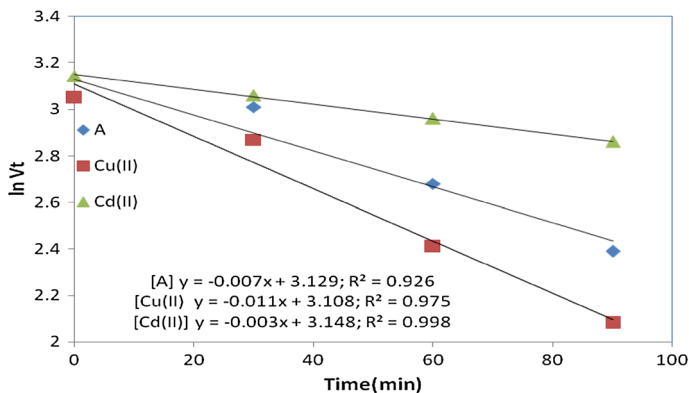


Fig. 1 Plots of $\ln V_t$ versus time for the formylation of phenol using $(\text{POCl}_3 + \text{DMF})$ at 333 K

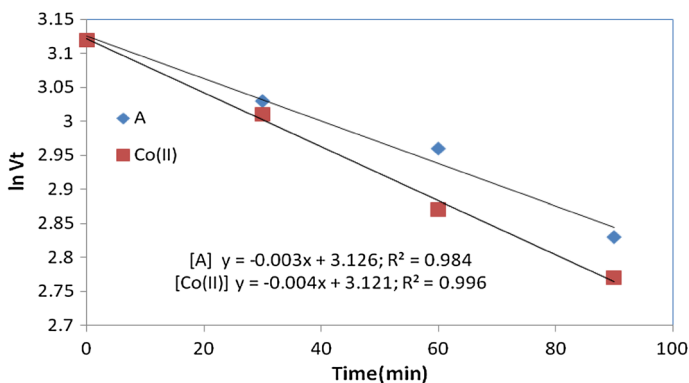


Fig. 2 Plots of $\ln V_t$ versus time for the formylation of naphthol using $(\text{SOCl}_2 + \text{DMF})$ at 333 K

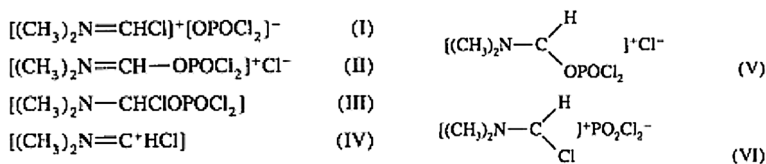
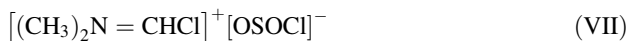


Chart 1 H reactive species with DMF POCl_3

kinetic studies reported from our laboratory [11, 12] on VH adducts, revealed that a number of covalent, ionic and ion-pair species of VH-adduct (I to VI) can exist in solution as shown in Chart 1, taking DMF and POCl_3 as a specific example (Chart 1).

Thionyl chloride, being a good Lewis acid like POCl_3 , can easily interact with a Lewis base (DMF) to form VH adducts analogous to DMF/ POCl_3 . In view of this, the reaction mechanism with DMF/ SOCl_2 does not differ much from that with DMF/ POCl_3 . It is therefore reasonable to consider similar type of reactive species (VII to X) in the present work. Accordingly, the species can be written as:



This aspect, coupled with the observed linearity of the plot of $\log_{10} k(\text{POCl}_3)$ versus $\log_{10} k(\text{SOCl}_2)$, indicates that a similar type of mechanism is operative in both the POCl_3 and SOCl_2 systems. Earlier studies from our laboratory also revealed that the reaction rates were relatively higher in DCE media (solvent of low dielectric constant) than those of MeCN media (solvent of high dielectric constant). Ingold's rule states that, for ion–ion and ion–dipole type species participating in the slow step, reaction rates should be faster in the solvent of low dielectric constant. This statement lends support for considering the participation of cationic species of VH adduct $(\text{Me}_2\text{N-CHCl})^+$ in the rate limiting step. In addition to this, the cationic species of VH adduct $(\text{Me}_2\text{N-CHCl})^+$ is electrophilically more reactive than non-ionic or ion-pair intermediates of the VH adduct (Scheme 2).

For the above scheme the rate law is,

Table 2 First-order rate constants for VH formylation with hydrocarbons

VH Reagent	Substrate	First order rate constant ($k' \times 10^{-5}$)/s ⁻¹				
		Native	Cu(II)	Ni(II)	Co(II)	Cd(II)
DMF/ POCl_3	Naphthalene	13.3	18.3	20.0	17.0	15.0
	Phenol	11.7	16.7	18.3	15.0	15.0
	4-Nitrophenol	5.00	6.67	6.67	6.70	12.0
	2-Chlorophenol	3.33	8.33	8.33	6.70	6.70
	<i>o</i> -Cresol	8.33	15.0	16.7	13.0	12.0
	<i>p</i> -Cresol	8.33	13.3	15.0	12.0	12.0
	Toluene	16.7	21.7	23.3	22.0	22.0
	Anisole	20.0	23.3	23.3	23.0	23.0
	1-Naphthol	13.3	18.3	20.0	18.0	18.0
	2-naphthol	13.3	23.3	23.3	23.0	22.0
DMF/ SOCl_2	Naphthalene	3.33	5.00	5.00	3.33	3.33
	Phenol	3.33	5.00	5.00	5.00	5.00
	4-Nitrophenol	1.67	3.33	1.67	1.67	1.67
	2-Chlorophenol	1.67	1.67	1.67	1.67	1.67
	<i>o</i> -Cresol	5.00	6.67	6.66	6.67	6.67
	<i>p</i> -Cresol	6.70	8.33	8.33	8.33	8.33
	Toluene	5.00	6.67	6.66	5.00	5.00
	Anisole	5.00	6.67	6.66	6.67	6.67
	1-Naphthol	5.00	5.00	6.66	5.00	5.00
	2-Naphthol	5.00	6.67	6.66	6.67	6.67

[subs] = 0.09 mol·dm⁻³; [VHR] = 0.005 mol·dm⁻³

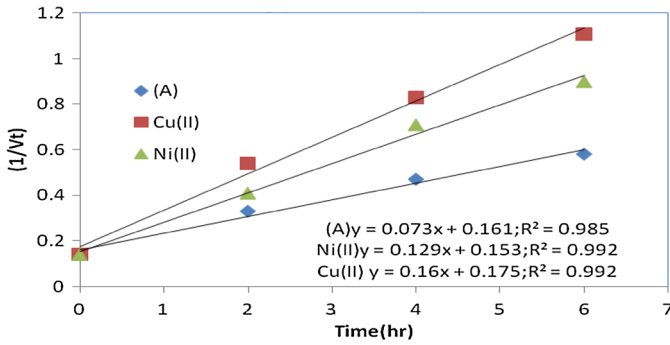


Fig. 3 Plots of $(1/V_t)$ versus time for the formylation of phenol using $(\text{POCl}_3 + \text{DMF})$ at 333 K

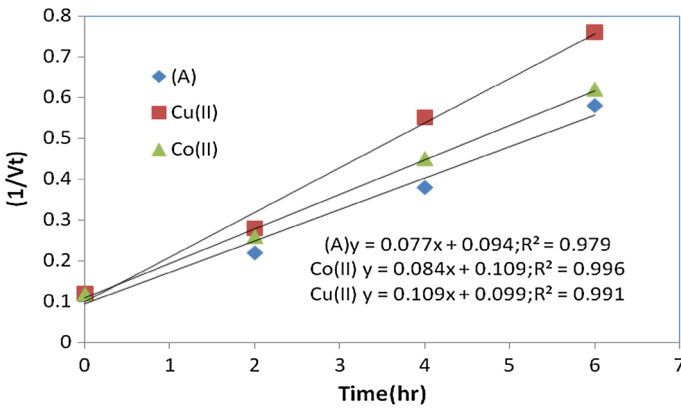
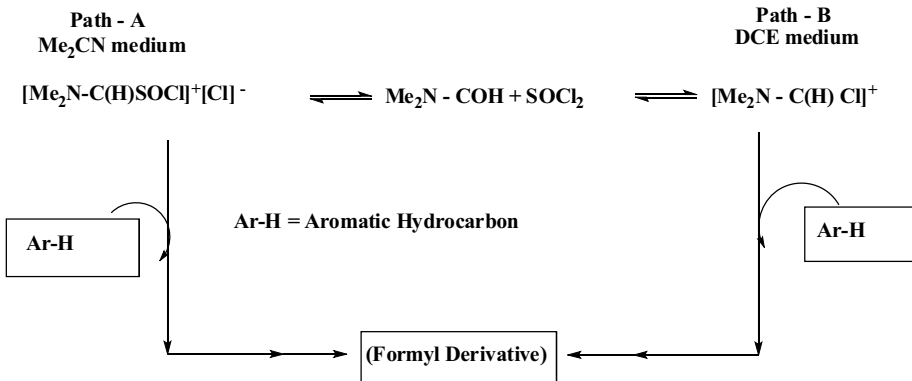


Fig. 4 Plots of $(1/V_t)$ versus time for the formylation of naphthol using $(\text{SOCl}_2 + \text{DMF})$ at 333 K



Scheme 2 General mechanism of VH formylation reactions

$$\frac{-d[\text{substrate}]}{dt} = k[\text{substrate}][\text{VH adduct}]$$

This rate law explains second-order kinetics with first-order dependences on [substrate] and [VH adduct], showing the consistency of the proposed mechanism.

3.1.2 Mechanism of VH Reactions in Transition Metal Ion Catalyzed Reactions

In order to have a closer look into the transition metal ion catalyzed reactions, a detailed spectrophotometric study dealing with M(II) binding with the substrate and VHR under different conditions has been undertaken. Electronic absorption spectra of Cu(II), Ni(II) and Co(II) showed bands at 756, 490 and 512 nm, respectively. These bands underwent either hypsochromic or bathochromic shifts in the presence of aromatic hydrocarbon, with or without VHR. Observed shifts are shown in Figs. 5, 6, 7, 8 and the data are presented in Table 3. These observations indicate binary and ternary complex formation due to the interaction of substrate with metal ion M(II) in the absence and/or presence of VHR.

3.1.3 Metal Ion–Substrate Interactions



According to this model, a metal ion–substrate complex [M(II)S] is formed in the pre-equilibrium step due to the interaction of metal ion (M) with substrate (S). The equilibrium constant K or (K_1) is the binding constant, which can be determined using an approach of Benesi and Hildebrand [34–41]:

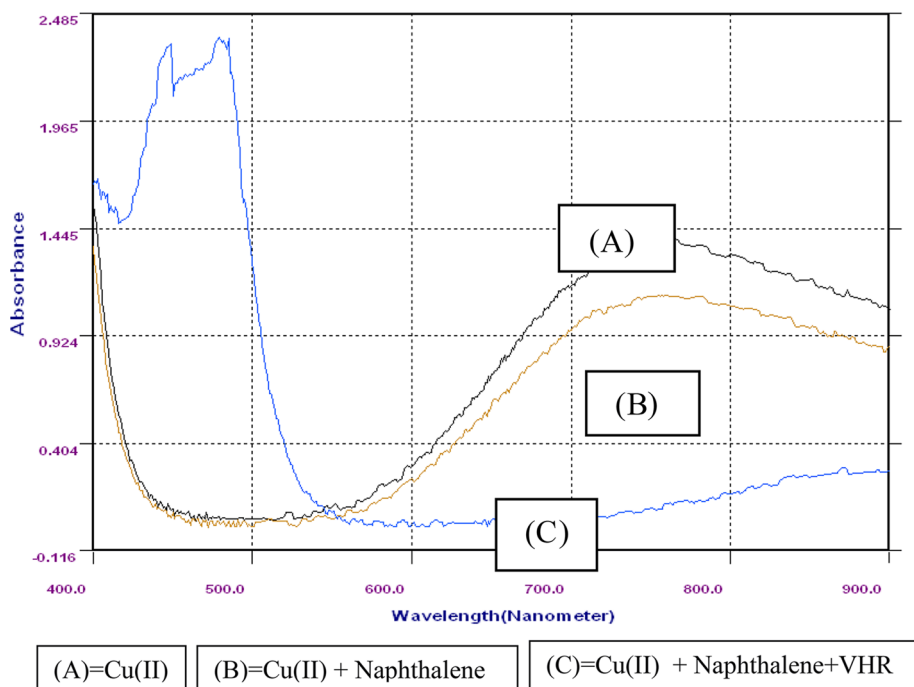


Fig. 5 UV–Visible spectra of Cu(II) with naphthalene and VHR

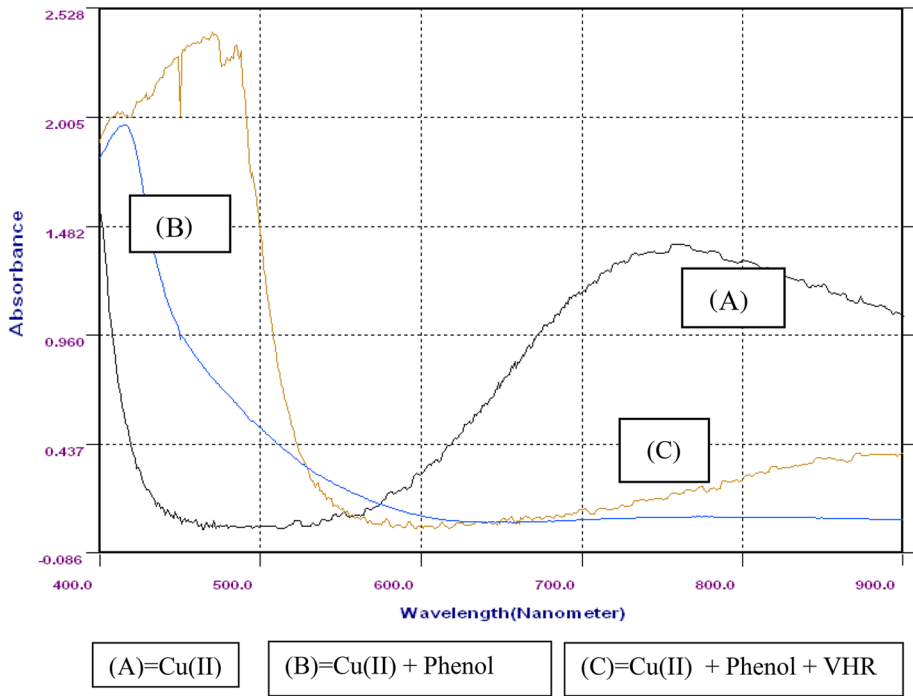


Fig. 6 UV–Visible spectra of Cu(II) with phenol and VHR

$$\Rightarrow [M(II)S] = \frac{K_1 [M(II)]C_S}{1 + K_1 [M(II)]} \tag{1}$$

where the total concentration of substrate is C_S , which is also considered as the algebraic sum of free substrate species (S) and metal ion bound substrate species (M(II)S). To observe one-to-one binding between a single substrate (S) and metal ion (M) using UV–V is absorbance, the Benesi–Hildebrand method [34–36] can be now employed. Using the Beer–Lambert law, the concentration of [M(II)S] can be rewritten as,

$$A = \varepsilon[M(II)S]b \text{ (where } b = \text{ path length)}$$

where $[M(II)S] = A/\varepsilon b$; when $b = 1 \text{ cm}$, $[M(II)S] = A/\varepsilon$.

Substituting for [M(II)S] in the binding isotherm Eq. 1, the equilibrium constant K can now be correlated to the change in absorbance due to the formation of the M(II)S complex.

$$\rightarrow \frac{A}{\varepsilon} = [M(II)S] = \frac{K[M(II)]C_S}{1 + K[M(II)]}$$

$$\Rightarrow \frac{A}{C_S} = [M(II)S] = \frac{\Delta\varepsilon K[M(II)]}{1 + K[M(II)]}$$

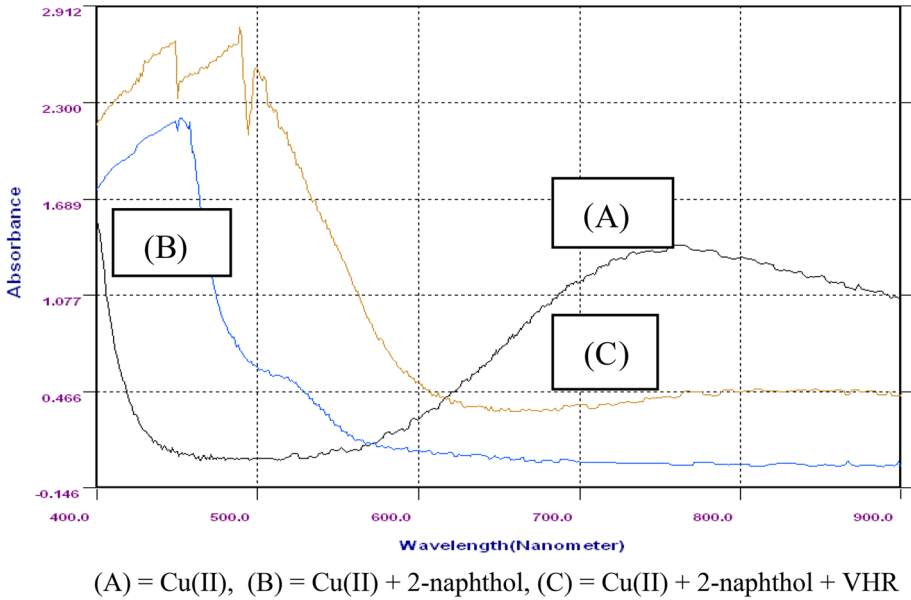


Fig. 7 UV-Visible spectra of Cu(II) with 2-naphthol and VHR

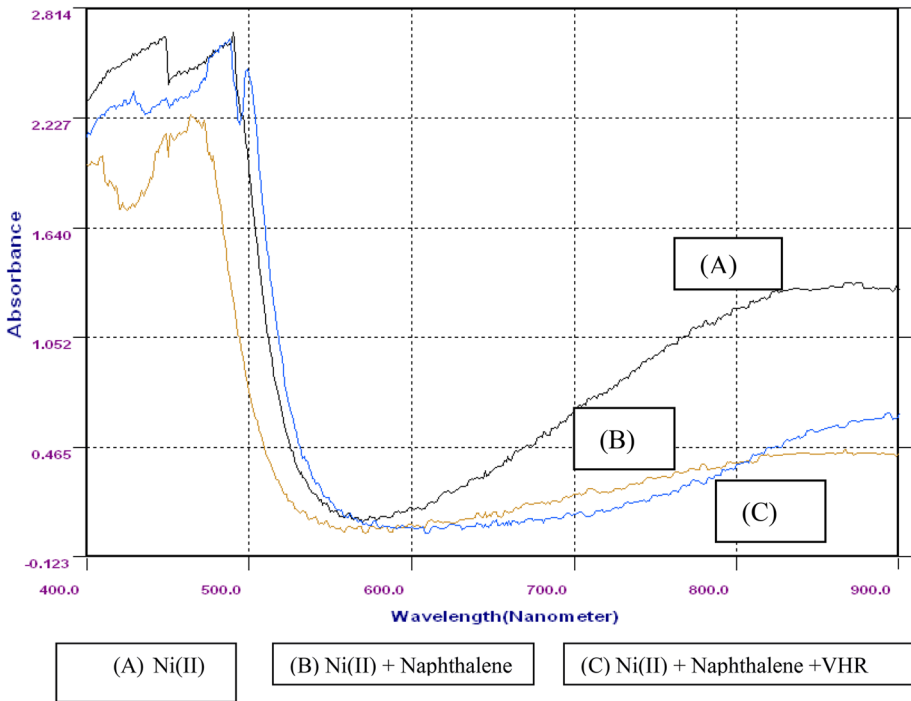


Fig. 8 UV-Visible spectra of Ni(II) with naphthalene and VHR

Table 3 UV spectroscopic observations of transition metal species in VH reactions

S. N.	Substrate	Metal ion	M(II) ion peak (nm)	M(II) + substrate peak(nm)	M(II) + substrate +VHR peak (nm)
1.	Naphthalene	Cu(II)	756	757 (slight bathochromic)	479 (hypsochromic)
		Ni(II)	490	462 (hypsochromic)	499 (bathochromic)
		Co(II)	520	510 (hypsochromic)	588, 684 (bathochromic)
2.	Phenol	Cu(II)	756	415 (hypsochromic)	470 (hypsochromic)
		Ni(II)	490	470 (hypsochromic)	499 (bathochromic)
		Co(II)	520	517 (hypsochromic)	589,685 (bathochromic)
3.	2-Naphthol	Cu(II)	756	453 (hypsochromic)	489 (hypsochromic)
		Ni(II)	490	464 (hypsochromic)	498 (bathochromic)
		Co(II)	520	510 (hypsochromic)	587,654 (bathochromic)
4.	Toluene	Cu(II)	756	748 (hypsochromic)	470 (hypsochromic)
		Ni(II)	490	463 (hypsochromic)	497 (bathochromic)
		Co(II)	520	517 (hypsochromic)	589, 685 (bathochromic)

$$\Rightarrow \frac{C_s}{A} = \frac{1}{\epsilon K[M(II)]} + \frac{1}{\epsilon}$$

Further modifications result in an equation where a double reciprocal plot can be made with (C_s/A) as a function of $1/[M(II)]$, and the value of ϵ can be derived from the intercept while K can be calculated from the slope. Such reciprocal plots have been made in this study and can be seen in Fig. 9. The values of K and ϵ are presented in Table 4.

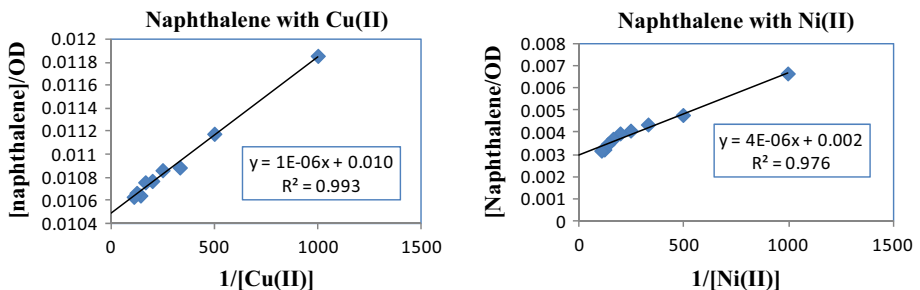


Fig. 9 Benesi–Hildebrand plots for K_1

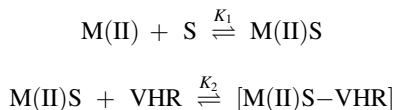
Table 4 Computation of formation constants of [M(II)-S] complexes

System	System	Peak (nm)	Type of Shift	Benesi-Hildebrand equation	K_1 or K_2	ϵ	$\Delta G/\text{kJ}\cdot\text{mol}^{-1}$
Binary K_1	Cu(II) + naphthalene	757	Bathochromic	$y = 3 \times 10^{-5}x + 0.016$; $R^2 = 0.97$	533	62.5	-16
	Ni(II) + naphthalene	462	Hypsochromic	$y = 4 \times 10^{-6}x + 0.002$; $R^2 = 0.976$	500	500	-15
	Co(II) + naphthalene	510	Hypsochromic	$y = 6 \times 10^{-6}x + 0.004$; $R^2 = 0.983$	666	250	-16
	Cu(II) + 2-naphthol	453	Hypsochromic	$y = 7 \times 10^{-6}x + 0.003$; $R^2 = 0.976$	428	333.3	-15
	Ni(II) + 2-naphthol	464	Hypsochromic	$y = 9 \times 10^{-6}x + 0.002$; $R^2 = 0.989$	222	500	-13
Ternary K_2	Co(II) + 2-naphthol	510	Hypsochromic	$y = 3 \times 10^{-6}x + 0.007$; $R^2 = 0.945$	2330	142.8	-19
	Cu(II) + naphthalene + VHR	479	Hypsochromic	$y = 2 \times 10^{-5}x + 0.001$; $R^2 = 0.998$	1.87	50.0	-2
	Ni(II) + naphthalene + VHR	499	Bathochromic	$y = 6 \times 10^{-7}x + 0.003$; $R^2 = 0.969$	200	16.66	-13
	Co(II) + naphthalene + VHR	588,684	Bathochromic	$y = 2 \times 10^{-6}x + 0.001$; $R^2 = 0.935$	18.76	40.0	-7
	Cu(II) + 2-naphthol + VHR	489	Hypsochromic	$y = 6 \times 10^{-6}x + 0.002$; $R^2 = 0.984$	15.5	25.0	-7
	Ni(II) + 2-naphthol + VHR	498	Bathochromic	$y = 6 \times 10^{-6}x + 0.0009$; $R^2 = 0.973$	135.14	55.55	-12
	Co(II) + 2-naphthol + VHR	587,654	Bathochromic	$y = 3 \times 10^{-6}x + 0.001$; $R^2 = 0.949$	2.86	50.0	-3

Error limits for formation constant K_1 and $K_2 = \pm 5$ to 10 units, for $\Delta G = \pm 3$ to 5 $\text{kJ}\cdot\text{mol}^{-1}$

3.1.4 Interaction of Metal ion with Substrate in the Presence of VHR

The model for ternary complex formation in micellar media is represented in the following equilibria:



The terms M, S and VHR represent metal ion, substrate, brominating reagent in these equations while [M(II)S] and [M(II)S–VHR] refer to binary and ternary complexes formed due to the interaction of metal ion, substrate, and VHR respectively:

$$[M(II)S-VHR] = K_2[M(II)S][VHR]$$

$$[M(II)S] = K_1[M(II)][S] \Rightarrow [S] = [M(II)S]/K_1[M(II)]$$

However, the total substrate concentration ([S]_t) is the sum of free substrate (S) and metal ion bound substrate (M(II)S) concentrations, respectively:

$$[S]_t = [S] + [M(II)S] \Rightarrow [S] = [S]_t - [M(II)S]$$

Application of the equilibrium concept finally leads to an expression for [M(II)S-VHR]:

$$[M(II)S - VHR] = \frac{K_1 K_2 [M(II)] [S]_t [VHR]_t}{(1 + K_1 [M(II)] + K_1 K_2 [M(II)] [S]_t)} \tag{2}$$

Using the Beer–Lambert law, this equation can be rewritten with the absorption coefficients and concentrations of each component:

$$A = \varepsilon[(M(II)S - VHR)]b \text{ (where } b = \text{ path length)}$$

where [(M(II)S-VHR)] = A/εb; when b = 1 cm, [M(II)S] = A/ε. Substituting for [(M(II)S-VHR)] in the binding isotherm Eq. 2, the equilibrium constant K can now be correlated to the change in absorbance due to the formation of the [(M(II)S-VHR)] complex:

$$A = \frac{\varepsilon(K_1 K_2 [M(II)] [S]_t [VHR]_t)}{(1 + K_1 [M(II)] + K_1 K_2 [M(II)] [S]_t)} = \frac{\varepsilon(K_1 K_2 [M(II)] [S]_t [VHR]_t)}{1 + K_1 [M(II)] (1 + K_2 [S]_t)}$$

Taking reciprocals to the above equation affords a reciprocal plot with (1/A) as a function of 1/[M(II)], and ε can be derived from the intercept while K can be calculated from the slope:

$$\frac{1}{A} = \frac{1 + K_1 [M(II)] (1 + K_2 [S]_t)}{\varepsilon(K_1 K_2 [M(II)] [S]_t [VHR]_t)}$$

$$\frac{1}{A} = \frac{1}{\varepsilon(K_1 K_2 [M(II)] [S]_t [VHR]_t)} = \frac{(1 + K_2 [S]_t)}{\varepsilon(K_2 [S]_t [VHR]_t)}$$

$$\frac{[S]_t [VHR]_t}{A} = \frac{1}{\varepsilon(K_1 K_2 [M(II)])} = \frac{(1 + K_2 [S]_t)}{\varepsilon K_2}$$

Now, from the reciprocal plot with $([S]_t[VHR]_t/\Delta A)$ as a function of $1/[M(II)]$, a straight line with intercept $(1 + K_2[S]_t)/\varepsilon K_2$ and slope $= (1/\varepsilon K_1 K_2)$ should be obtained, which is observed in the present study (Fig. 10). From the intercept, the value ε can be computed with the assumption that $1 \ll K_2[S]_t$, which ultimately leads to intercept $= [S]_t/\varepsilon$, while K_2 can be calculated from the slope with proper substitution of K_1 evaluated earlier for the binary system. Gibbs energy values (ΔG) involving the formation constants (K_1 and K_2) are evaluated according to van't Hoff's isotherm, and related data are presented in Table 4:

$$\Delta G = -RT \ln K_i.$$

3.1.5 Metal Ion Catalyzed Mechanism of Formylation Reactions Involving a DMF–Oxychloride $[POCl_3$ or $SOCl_2$] Adduct

UV spectroscopic studies (Figs. 5, 6, 7 and 8) of metal ion interactions with aromatic hydrocarbons and in the absence and presence of VH reagents clearly indicate that aromatic hydrocarbons form binary $[M(II)S]$ complexes as well as ternary complexes of the type $[M(II)S-VHR]$. These findings, coupled with the observed second-order kinetics with first-order rate dependences on $[substrate]$ as well as $[VHR]$ and rate enhancements in metal ion catalyzed reactions, substantiate the formation of a binary $[M(II)S]$ complex in the first step giving rise to a ternary complex in the second step. The ternary complex thus formed rearranges to give products in the slow step, as is shown in Schemes 3 and 4.

In Schemes 3 and 4, $[M(II)S]$ and $[M(II)S-VHR]$ refer to binary and ternary complexes formed due to the interaction of metal ion, substrate, and VHR, respectively. The products are obtained from the decomposition of $[M(II)S-VHR]$ in the slow step in the metal ion catalyzed reactions. For the above schemes the rate law is given by:

$$\Rightarrow V = \frac{k_c K_1 K_2 [M(II)]_t [S]_t [VHR]_t}{(1 + K_1 [M(II)]_t + K_1 K_2 [M(II)]_t [S]_t)}$$

According to this rate law, the reaction kinetics should indicate first-order kinetics with respect to $[VHR]$ and fractional order in both $[substrate]$ as well as $[M(II)]$. But, the kinetics of the study indicate first order in both the reactants $[VHR]$ and $[substrate]$. This change may be explained due to the small contribution of the product of $(K_1 K_2 [M(II)]_t [S]_t)$. If $(1 + K_1 [M(II)]_t) \gg K_1 K_2 [M(II)]_t [S]_t$ in the denominator of the above rate equation, then the contribution of $(K_1 K_2 [M(II)]_t [S]_t)$ can be neglected. The rate equation now takes the form,

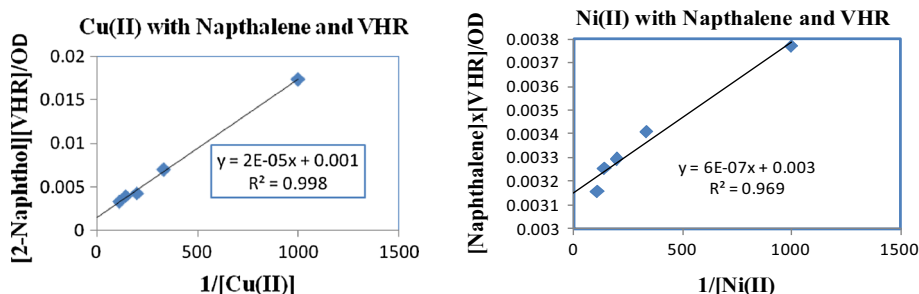
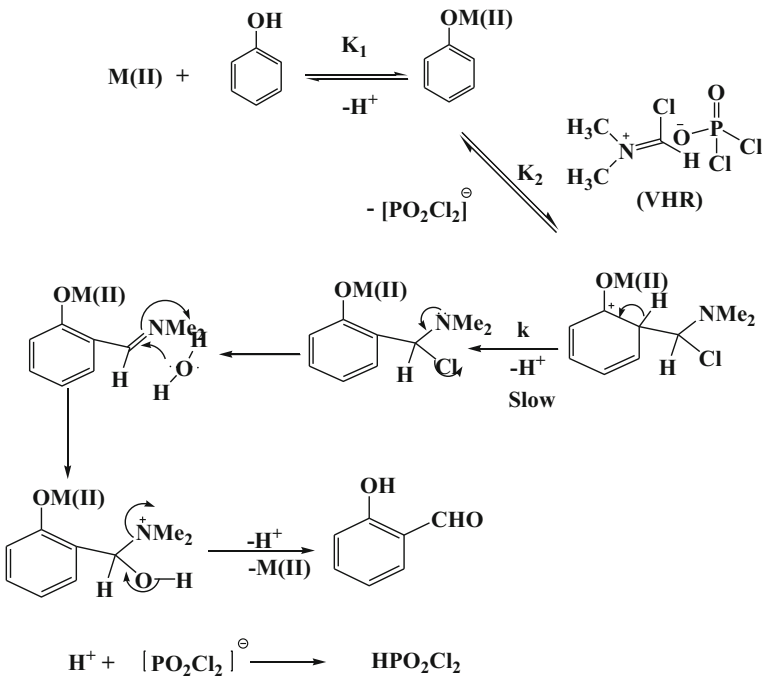
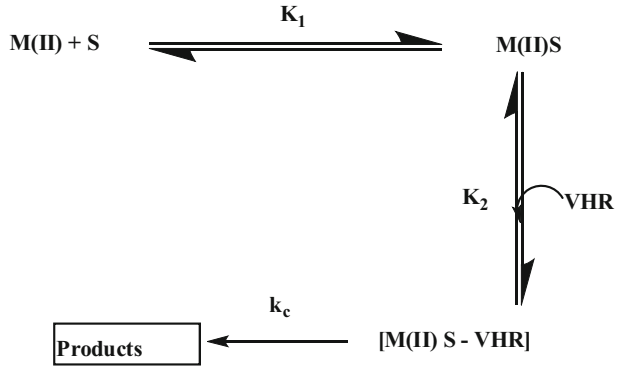


Fig. 10 Benesi–Hildbrand plots for K_2

Scheme 3 Metal ion catalyzed VH reaction with hydrocarbons



Scheme 4 Metal ion catalyzed VH mechanism with phenol

$$V = \frac{k_c K_1 K_2 [M(II)] [S]_t [VHR]_t}{1 + K_1 [M(II)]}$$

Rearranging the rate law gives:

$$\frac{V}{[S]_t [VHR]_t} = k'' = \frac{k_c K_1 K_2 [M(II)]}{1 + K_1 [M(II)]}$$

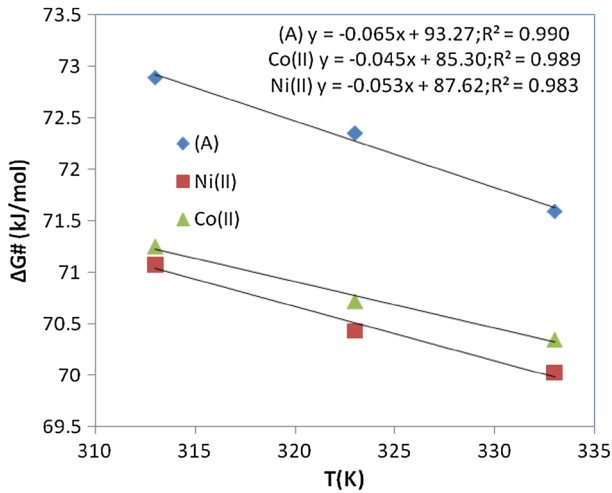


Fig. 11 Gibbs–Helmholtz plots for VH formylation of phenol using ($POCl_3 + DMF$)

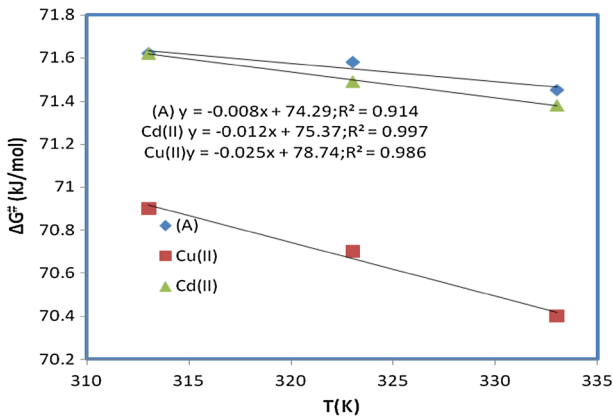


Fig. 12 Gibbs–Helmholtz plots for VH formylation of 1-naphthol using ($SOCl_2 + DMF$)

Since very low concentrations ($[M(II)] < 0.001 \text{ mol}\cdot\text{L}^{-1}$) are used in this study, the contribution due to ($K_1 [M(II)]$) can be neglected in the denominator. The above equation then takes the form,

$$k'' = k_c K_1 K_2 [M(II)]$$

Second-order rate constants (k'') are reported in Table 4 and related activation parameters were computed from Eyring's equation using the theory of reaction rates [37, 38]. According to Eyring's theory of reaction rates, the rate constant (k) can be given as

$$k = (k_t) (RT/Nh) \exp(-\Delta G^\ddagger / RT) \quad (3)$$

In the above equation, the transmission coefficient (k_t) is assumed to be unity; R , N , h and T represent the gas constant, Avogadro number, Planck's constant and reaction

Table 5 Temperature dependant second-order rate constants for VH formylation reactions with aromatic hydrocarbons in ACN solvent

Substrate	Temp. (K)	$k' \times 10^{-4}/\text{dm}^3 \cdot \text{mol}^{-1} \cdot \text{s}^{-1}$ (POCl ₃ + DMF) system				$k'' \times 10^{-4}/\text{dm}^3 \cdot \text{mol}^{-1} \cdot \text{s}^{-1}$ (SOCl ₂ + DMF) system				
		Native	Cu(II)	Ni(II)	Cd(II)	Native	Cu(II)	Ni(II)	Cd(II)	
Naphthalene	313	6.16	19.04	17.92	15.12	4.48	6.7	6.7	5.0	6.2
	323	18.48	47.6	43.12	37.52	12.88	17.4	19.0	13.4	15.7
	333	50.4	103.04	118.16	89.6	34.72	54.9	49.3	45.4	42.6
Phenol	313	4.48	9.52	8.96	8.4	5.6	8.4	7.8	7.8	7.3
	323	13.44	33.04	27.44	24.64	14.56	22.4	21.8	19.6	18.5
	333	40.88	89.04	72.24	64.96	34.16	56.6	56.6	48.2	44.2
4-Nitrophenol	313	7.28	15.68	11.2	14.0	3.92	4.5	6.7	5.6	3.9
	323	20.16	37.52	28.56	33.6	12.32	19.6	17.4	14.6	15.1
	333	52.08	104.7	65.52	89.6	31.36	52.1	41.4	34.7	42.0
2-Chloro phenol	313	11.2	21.8	20.16	17.36	3.9	5.0	6.2	4.5	3.9
	323	28.56	53.2	48.72	45.36	11.2	15.7	15.7	14.6	14.0
	333	71.12	120.4	110.3	105.8	33.6	53.2	43.7	38.6	39.8
<i>o</i> -Cresol	313	7.84	14.0	14.0	11.2	4.48	6.7	6.7	6.2	5.6
	323	20.16	35.28	34.16	29.12	12.32	19.6	17.9	16.2	14.0
	333	49.28	90.72	90.72	66.64	32.48	47.0	43.1	47.6	38.0
<i>p</i> -Cresol	313	8.4	14.56	13.44	12.88	4.48	7.3	7.3	6.2	6.2
	323	24.08	41.44	38.64	36.96	12.32	18.5	17.9	16.2	16.2
	333	70	101.92	90.16	87.36	30.8	46.5	43.7	42.6	43.1
Toluene	313	4.4	9.52	7.28	6.72	3.36	3.9	3.4	3.4	4.5
	323	15.68	29.68	28.56	24.64	8.9	12.9	11.8	12.3	11.2
	333	39.2	84.0	68.32	61.6	22.4	43.1	38.1	39.8	28.0
Anisole	313	6.72	11.76	11.2	10.64	6.16	9.0	7.8	8.4	7.3
	323	16.8	35.28	30.8	26.88	17.36	29.7	29.7	26.9	21.3
	333	45.36	104.16	79.52	70.56	48.16	68.3	76.7	67.8	52.6

Table 5 continued

Substrate	Temp. (K)	$k'' \times 10^{-4}/\text{dm}^3 \cdot \text{mol}^{-1} \cdot \text{s}^{-1}$ ($\text{POCl}_3 + \text{DMF}$) system				$k'' \times 10^{-4}/\text{dm}^3 \cdot \text{mol}^{-1} \cdot \text{s}^{-1}$ ($\text{SOCl}_2 + \text{DMF}$) system					
		Native	Cu(II)	Ni(II)	Co(II)	Cd(II)	Native	Cu(II)	Ni(II)	Co(II)	Cd(II)
1-Naphthol	313	6.16	12.88	11.2	9.52	8.4	7.28	9.5	10.1	9.5	8.4
	323	16.24	31.92	27.44	22.96	21.28	17.92	24.6	26.3	25.2	20.7
	333	40.32	72.24	70.5	55.44	50.96	43.12	61.0	61.6	60.5	51.0
2-Naphthol	313	8.96	10.64	10.08	10.08	13.4	7.28	12.9	10.6	10.1	9.0
	323	24.64	47.6	43.68	40.32	37.52	19.04	32.5	28.0	26.9	24.0
	333	64.1	120.4	100.8	91.8	91.8	45.36	81.2	72.2	64.4	57.7

Error limits for second-order rate constant: ± 0.10 units

Table 6 Temperature dependent Gibbs energies of activation for VH formylation reactions with aromatic hydrocarbons in ACN solvent

Substrate	$\Delta G^\ddagger/\text{kJ}\cdot\text{mol}^{-1}$ (POCl ₃ + DMF) system				$\Delta G^\ddagger/\text{kJ}\cdot\text{mol}^{-1}$ (SOCl ₂ + DMF) System						
	Temp (K)	Native	Cu(II)	Ni(II)	Co(II)	Cd(II)	Native	Cu(II)	Ni(II)	Co(II)	Cd(II)
Naphthalene	313	72.06	69.13	69.28	69.72	70.38	72.8	71.84	71.8	72.6	72.04
	323	71.49	68.95	69.22	69.59	69.89	72.4	71.66	72.2	72.3	71.93
	333	71.01	68.66	68.66	69.42	69.85	72.1	70.78	71.0	71.3	71.48
Phenol	313	72.89	70.92	71.08	71.25	71.62	72.3	71.25	71.4	71.4	71.62
	323	72.35	69.93	70.43	70.72	71.42	72.1	70.98	71.0	71.3	71.49
	333	71.59	69.44	70.02	70.31	70.64	72.1	70.69	70.6	71.1	71.38
4-nitro phenol	313	71.62	69.63	70.50	69.92	70.93	73.2	72.87	71.8	72.3	73.25
	323	71.26	69.59	70.33	69.89	70.79	72.6	71.34	71.6	72.1	72.04
	333	70.92	68.99	70.29	69.42	70.16	72.3	70.92	71.5	72	71.52
2-chloro phenol	313	70.5	68.76	68.97	69.36	69.92	73.2	72.6	72.0	72.8	73.25
	323	70.33	68.65	68.89	69.08	69.33	72.8	71.93	71.9	72.1	72.24
	333	70.06	68.60	68.85	68.96	68.99	72.1	70.8	71.4	71.7	71.67
<i>O</i> -cresol	313	71.43	69.92	69.92	70.50	70.50	72.9	71.8	71.8	72	72.31
	323	71.26	69.76	69.84	70.27	70.49	72.6	71.3	71.5	71.8	72.24
	333	71.08	69.39	69.39	70.24	70.24	72.2	71.2	71.4	71.1	71.8
<i>P</i> -cresol	313	71.25	69.82	70.03	70.14	70.38	72.9	71.6	71.6	72.04	72.04
	323	70.78	69.33	69.51	69.63	69.89	72.6	71.4	71.5	71.85	71.85
	333	70.11	69.07	69.40	69.49	69.76	72.4	71.2	71.4	71.48	71.45
Toluene	313	72.93	69.82	71.62	71.83	72.89	73.6	73.2	73.6	73.6	72.87
	323	71.94	68.74	70.33	70.72	71.12	73.5	72.4	72.7	72.5	72.84
	333	71.71	68.53	70.17	70.46	70.67	73.3	71.4	71.7	71.6	72.64
Anisole	313	71.8	70.38	70.50	70.64	70.78	72.1	71	71.4	71.2	71.62
	323	71.7	69.76	70.12	70.49	70.61	71.7	70.2	70.2	70.4	71.11
	333	71.31	69.01	69.75	70.08	70.32	71.1	70.1	69.8	70.1	70.90

Table 6 continued

Substrate	Temp (K)	$\Delta G^\ddagger/\text{kJ}\cdot\text{mol}^{-1}$ ($\text{POCl}_3 + \text{DMF}$) system					$\Delta G^\ddagger/\text{kJ}\cdot\text{mol}^{-1}$ ($\text{SOCl}_2 + \text{DMF}$) System				
		Native	Cu(II)	Ni(II)	Co(II)	Cd(II)	Native	Cu(II)	Ni(II)	Co(II)	Cd(II)
1-Naphthol	313	72.06	70.14	70.50	70.92	71.25	71.6	70.9	70.7	70.9	71.25
	323	71.84	70.03	70.43	70.91	71.12	71.6	70.7	70.5	70.6	71.19
	333	71.63	70.02	70.09	70.75	70.99	71.4	70.4	70.4	70.5	70.98
2-Naphthol	313	71.08	70.64	70.78	70.78	70.04	71.6	70.9	70.6	70.7	71.00
	323	70.72	68.95	69.18	69.40	69.59	71.4	69.9	70.3	70.4	70.70
	333	70.35	68.60	69.10	69.35	69.36	71.3	69.6	70.2	70.3	70.60

Error limits for $\Delta G^\ddagger = \pm 2.0$ to $3.0 \text{ kJ}\cdot\text{mol}^{-1}$

Table 7 Enthalpy and entropy of activation parameters for formylation of hydrocarbons with VH reagents

VH Reagent	Substrate	Enthalpy of activation $\Delta H^\ddagger/\text{kJ}\cdot\text{mol}^{-1}$				Entropy of activation $\Delta S^\ddagger/\text{J}\cdot\text{K}^{-1}\cdot\text{mol}^{-1}$					
		Native	Cu(II)	Ni(II)	Co(II)	Native	Cu(II)	Ni(II)	Co(II)	Cd(II)	
DMF/POCl ₃	Naphthalene	88.47	76.5	79.06	74.3	77.28	52.0	23.0	31.0	15.0	22.0
	Phenol	93.27	93.99	87.62	85.36	87.05	65.0	74.0	53.0	45.0	49.0
	4-Nitrophenol	82.24	79.73	78.34	77.77	83.48	34.0	32.0	25.0	25.0	40.0
	2-Chlorophenol	78.34	71.25	69.68	75.52	85.51	25.0	8.0	2.00	20.0	50.0
	<i>o</i> -Cresol	76.9	78.25	79.35	74.53	75.21	17.0	26.0	30.0	13.0	15.0
	<i>p</i> -Cresol	88.3	81.51	79.32	81.0	79.62	54.0	37.0	30.0	35.0	30.0
	Toluene	91.38	89.99	94.89	93.67	107	59.0	65.0	75.0	70.0	11.0
	Anisole	79.69	91.84	83.02	80.0	77.0	25.0	68.0	40.0	30.0	20.0
	1-Naphthol	78.77	71.34	76.96	73.6	75.9	21.0	4.0	20.0	8.00	15.0
	2-Naphthol	81.97	101.6	85.61	87.4	80.9	35.0	10.0	50.0	55.0	35.0
DMF/SOCl ₂	Naphthalene	86.03	88.54	84.32	93.06	81.45	42.0	53.0	40.0	65.0	30.0
	Phenol	75.03	80.01	83.17	76.11	75.37	11.0	28.0	37.0	15.0	12.0
	4-Nitrophenol	87.20	103.2	76.47	76.97	99.68	45.0	97.0	15.0	15.0	85.0
	2-Chlorophenol	90.46	99.88	81.45	89.96	98.17	55.0	87.0	30.0	55.0	80.0
	<i>o</i> -cresol	81.71	81.12	78.02	86.16	80.17	28.0	30.0	20.0	45.0	25.0
	<i>p</i> -Cresol	80.60	77.86	74.73	81.42	81.42	25.0	20.0	10.0	30.0	30.0
	Toluene	79.86	101.4	103.3	104.8	76.49	20.0	90.0	95.0	100	11.0
	Anisole	86-10	84-96	96.3	88.33	82.83	45.0	45.0	80.0	55.0	36.0
	1-Naphthol	74.73	78.74	75.37	77.12	75.50	10.0	25.0	15.0	20.0	13.0
	2-Naphthol	76.27	77.94	79.99	76.92	77.77	15.0	25.0	30.0	20.0	21.0

Error limits for $\Delta H^\ddagger = \pm 2.0$ to $3.0 \text{ kJ}\cdot\text{mol}^{-1}$ and for $\Delta S^\ddagger = \pm 5.0$ to $6.0 \text{ J}\cdot\text{K}^{-1}\cdot\text{mol}^{-1}$

temperature, and ΔG^\ddagger the Gibbs energy of activation. Rearrangement of the above equation gives:

$$\exp(\Delta G^\ddagger/RT) = (RT/Nhk) \quad (4)$$

Taking the natural logarithm for the above equation then gives:

$$\Delta G^\ddagger = RT \ln (RT/Nhk) \quad (5)$$

The Gibbs energy of activation (ΔG^\ddagger) has been evaluated at various temperatures by using the above equation. But, the Gibbs energy of activation (ΔG^\ddagger) is related to the enthalpy (ΔH^\ddagger) and entropy of activation (ΔS^\ddagger) by the Gibbs–Helmholtz equation:

$$\Delta G^\ddagger = \Delta H^\ddagger - T\Delta S^\ddagger \quad (6)$$

Now, the plots of ΔG^\ddagger as a function of temperature (T) should be linear with negative slopes (ΔS^\ddagger) and definite intercepts on the ordinate which are equal to (ΔH^\ddagger). Such plots were realized in the present study (Figs. 11 and 12). From the slopes and intercepts of these plots, the enthalpies and entropies of activation were evaluated. Activation parameters have been evaluated for all the substrates studied in this reaction and the data are presented in Tables 5, 6 and 7. It is of interest to note that Gibbs energies of activation (ΔG^\ddagger) for all the substrates are by and large of the same magnitude, indicating a similar type of mechanism is operative. The small entropies of activation (ΔS^\ddagger) presented in these tables show that the transition state is tending towards decomposition to afford stable products. Obtained negative Gibbs energy values (ΔG) for binding constants K_1 and K_2 indicate the favorable nature of complex formation during the course of the reaction.

4 Conclusions

In summary, the authors have successfully demonstrated transition metal ion catalyzed Vilsmeier–Haack formylation reactions with hydrocarbons in acetonitrile medium. The VH reactions followed second-order kinetics and afford formyl derivatives under kinetic conditions, also irrespective of the nature of oxychloride used for the preparation of VH reagent along with DMF. The calculated Gibbs energies of activation (ΔG^\ddagger) for all the substrates are, by and large, of the same magnitude, indicating a similar type of mechanism is operative. Small positive entropies of activation (ΔS^\ddagger) observed in this study probably indicate that the transition state is tending towards decomposition to afford stable products. The obtained negative Gibbs energy values (ΔG) for binding constants K_1 and K_2 indicate the spontaneous nature of complex formation during the course of reaction. The present finding is advantageous to understand the nature of reactive species as well as the mechanism of formylation.

Acknowledgments The authors thank Prof. P. K. Saiprakash (Former Dean, Science Faculty, O.U.), authorities of MJCET, and NIPER for constant encouragement.

References

1. Vilsmeier, A., Haack, A.: Vilsmeier–Haack reaction. *Ber. Bunsenges. Chem. Ges.* **60**, 119–122 (1927)
2. Meth-Cohn, O.: The Vilsmeier–Haack reaction. *Comp. Org. Syn.* **2**, 777–794 (1991)

3. Arnold, Z., Holy, A.: Synthetic reactions of dimethylformamide. XIV. Some new findings on adducts of the Vilsmeier–Haack type. *Collect. Czech. Chem. Commun.* **27**, 2886–2897 (1962)
4. Arnold, Z., Holy, A.: Synthetic reactions of dimethylformamide. XVIII. Reactivity of methyl groups in polymethinium salts. *Collect. Czech. Chem. Commun.* **28**, 2040–2046 (1963)
5. Smith, T.D.: The reaction of NN-dimethylformamide with phosphorus trichloride. *J. Chem. Soc. A* **7**, 841–842 (1966)
6. Martin, G.J., Poignant, S.: Nuclear magnetic resonance investigations of carbonium ion intermediates. Part I. Kinetics and mechanism of formation of the Vilsmeier–Haack reagent. *J. Chem. Soc. Perkin 2* 1964–1966 (1972)
7. Martin, G.J., Poignant, S.: Nuclear magnetic resonance investigations of carbonium ion intermediates. Part II. Exchange reactions in chloro-iminium salts (Vilsmeier–Haack reagents). *J. Chem. Soc. Perkin 2* 642–646 (1974)
8. Sethna, S.M., Shah, N.M.: The chemistry of coumarins. *Chem. Rev.* **36**, 1–62 (1945)
9. Alumi, S., Linda, P., Marino, G., Santine, S., Salvelli, G.: The mechanism of the Vilsmeier–Haack reaction. Part II. A kinetic study of the formylation of thiophen derivatives with dimethylformamide and phosphorus oxychloride or carbonyl chloride in 1,2-dichloroethane. *J. Chem. Soc Perkin 2* 2070–2073 (1972)
10. Linda, P., Luccarelli, A., Marino, G., Savelli, G.: The mechanism of the Vilsmeier–Haack reaction. Part III. Structural and solvent effects. *J. Chem. Soc. Perkin 2* 1610–1612 (1974)
11. Rajanna, K.C., Soloman, F., Moazzam Ali, M., Saiprakash, P.K.: Kinetics and mechanism of Vilsmeier–Haack synthesis of 3-formyl chromones derived from o-hydroxy aryl alkyl ketones: a structure reactivity study. *Tetrahedron* **52**, 3669–3682 (1996)
12. Rajanna, K.C., Soloman, F., Moazzam Ali, M., Saiprakash, P.K.: Vilsmeier–Haack formylation of coumarin derivatives. A solvent dependent kinetic study. *Int. J. Chem. Kinet.* **28**, 865–872 (1996)
13. Rajanna, K.C., Venkateswarlu, M., Satish Kumar, M., Umesh Kumar, U., Ramgopal, S., Saiprakash, P.K.: Kinetics and mechanism of certain acetylation reactions with acetamide/oxychloride in acetonitrile under Vilsmeier–Haack conditions. *Helv. Chim. Acta* **94**, 2168–2187 (2011)
14. Rajanna, K.C., Venkateswarlu, M., Satish Kumar, M., Umesh Kumar, U., Venkateswarlu, G., Saiprakash, P.K.: Kinetics and mechanism of certain benzoylation reactions under Vilsmeier–Haack conditions using benzamide and oxychloride in acetonitrile medium. *Int. J. Chem. Kinet.* **45**, 69–80 (2013)
15. Wynberg, H.: The Reimer–Tiemann reaction. *Chem. Rev.* **60**, 169–184 (1960)
16. Jack, L.J.: Name Reactions: A Collection of Detailed Reaction Mechanisms, 2nd edn, p. 157. Springer, New York (2003)
17. Ogata, Y., Sugiura, F.: Kinetics and mechanism of the Duff reaction. *Tetrahedron* **24**, 5001–5010 (1968)
18. Wiberg, N., Holleman, A.F., Wiberg, N.: *Holleman–Wiberg Inorganic Chemistry*, 34th edn. Academic Press, New York (2001)
19. Elschenbroich, Ch., Salzer, A.A.: *Organometallics*, 2nd edn. VCH, Weinheim (1992)
20. Thompson, D.T.: Some basic research in coordination chemistry and catalysis, related to applications for industry. *Coord. Chem. Rev.* **154**, 179–192 (1996)
21. Jagirdar, B.R.: Transition metal complexes and catalysis. *Resonance* **4**, 63–65 (1999)
22. Lakshmi, P.J., Rajanna, K.C., Saiprakash, P.K.: Mechanism of oxidation of iron(II) chelates by hexavalent chromium and heptavalent manganese in aqueous sulfuric acid and micellar media—a kinetic approach. *Transit. Met. Chem.* **21**, 135–141 (1996)
23. Reddy, K.N., Ram Reddy, M.K., Rajanna, K.C., Saiprakash, P.K.: A kinetic study of the 1,10-phenanthroline-catalysed iron(III) oxidation of epimeric *aldo*-, and *D*-, and *L*-keto-hexoses. *Transit. Met. Chem.* **21**, 112–116 (1996)
24. Reddy, J.N., Giridhar, S., Rajanna, K.C., Saiprakash, P.K.: Equilibrium and kinetic studies of electron transfer reactions involving quinolinium dichromate and amino alcohols in aqueous acid media. *Transit. Met. Chem.* **21**, 105–111 (1996)
25. Somaiah, P.V., Bal Reddy, K., Sethuram, B., Navaneeth Rao, T.: Kinetics and mechanism of oxidation of aryl β -styryl ketones by osmium tetroxide in sulphuric acid–acetic acid medium. A structure-reactivity correlation study. *Transit. Met. Chem.* **18**, 58–60 (1993)
26. Sondu, S., Sethuram, B., Rao, T.N.: Kinetics and mechanism of Rh(III)-catalysed oxidation of 1,2-glycols by acid bromate. *Transit. Met. Chem.* **15**, 78–80 (1990)
27. Sarala, G., Jayaprakash Rao, P., Sethuram, B., Navaneeth Rao, T.: Kinetics and mechanism of osmium(VIII)-catalyzed oxidation of phosphite by diperiodatoargentate(III) in alkaline medium. *Transit. Met. Chem.* **13**, 113–115 (1988)
28. Laxmi Venkat Rao, K., Prasada Rao, M., Sethuram, B., Navaneeth Rao, T.: Oxidations by iron(VI). Kinetic study of uncatalysed and osmium(VIII) catalysed oxidation of dimethyl sulphoxide in alkaline medium. *Transit. Met. Chem.* **14**, 165–168 (1989)

29. Lingamurthy, S., Sethuram, B., Navaneeth Rao, T.: Study of photoelectrochemical cells: micellar effect on the $[\text{Ru}(\text{bpy})_3]^{2+}$ -sensitized photoreduction of dyes by Na_2EDTA . *Transit. Met. Chem.* **17**, 506–508 (1992)
30. Ramesh, B., Sadanand, D.T., Gopikanth Reddy, S., Venkata Swamy, K., Saiprakash, P.K.: Hydrogenation of 1-alkenes catalysed by anchored montmorillonite palladium(II) complexes: a kinetic study. *Transit. Met. Chem.* **25**, 639–643 (2000)
31. Ramesh, K., Shylaja, S., Rajanna, K.C., Giridhar Reddy, P., Saiprakash, P.K.: Polyethylene glycol-mediated kinetic study of nitrodecarboxylation of α , β -unsaturated acids by Blau's Fe(III) bipy complex. *Int. J. Chem. Kinet.* **46**, 126–137 (2014)
32. Aneesa, F., Rajanna, K.C., Venkateswarlu, M., Rajendar Reddy, K., Arun Kumar, Y.: Efficient catalytic activity of transition metal ions in Vilsmeier-Haack reactions with acetophenones. *Int. J. Chem. Kinet.* **45**, 721–733 (2013)
33. Mendham, J., Denney, R.C., Barnes, J.D., Thomas, M.J.K.: *Vogel's Quantitative Chemical Analysis*, 6th edn. Prentice Hall, New York (2000)
34. Benesi, H., Hildebrand, J.: A spectrophotometric investigation of the interaction of iodine with aromatic hydrocarbons. *J. Am. Chem. Soc.* **71**, 2703–2707 (1949)
35. Rao, C.N.R.: *Ultraviolet and Visible Spectroscopy*. Butterworths, London (1961)
36. Ketelaar, J.A., von de Stolpe, C., Goud-Smit, A., Dzugas, W.: Spectrophotometric study of the solvation of iodine in dioxan solution II. *Rec. Trav. Chim* **71**, 1104–1114 (1952)
37. Laidler, K.J.: *Chemical Kinetics*, 3rd edn. Harper and Row, New York (1987)
38. Laidler, K.J., Meiser, J.H.: *Physical Chemistry*, 3rd edn. Houghton Mifflin, New York (1999)